



ELSEVIER

Journal of Chromatography A, 852 (1999) 59–71

JOURNAL OF  
CHROMATOGRAPHY A

# Use of surface plasmon resonance for studies of protein–protein and protein–phospholipid membrane interactions

## Application to the binding of factor VIII to von Willebrand factor and to phosphatidylserine-containing membranes

E. Saenko<sup>a,\*</sup>, A. Sarafanov<sup>a</sup>, N. Greco<sup>a</sup>, M. Shima<sup>b</sup>, K. Loster<sup>c</sup>, H. Schwinn<sup>d</sup>, D. Josic<sup>d</sup>

<sup>a</sup>Holland Laboratory, American Red Cross, Rockville, 15601 Crabbs Branch Way, Rockville, MD 20855, USA

<sup>b</sup>Department of Pediatrics, Nara Medical University, Kashihara City, Nara, Japan

<sup>c</sup>Free University of Berlin, Berlin, Germany

<sup>d</sup>Octapharma Pharmaceutica, Vienna, Austria

### Abstract

The surface plasmon resonance phenomenon is used for real time measurements of protein–protein and protein–membrane interactions. In the present study two surface plasmon resonance-based binding assays permitting study of the interaction of coagulation factor VIII (fVIII) with von Willebrand factor (vWf) and phospholipid have been developed. These interactions of fVIII are required for maintenance of fVIII concentration in circulation and for the assembly of the functional factor Xase complex, respectively. With these binding assays, the role of the light chain (LCh) in fVIII binding to vWf and to immobilized phospholipid monolayers and intact vesicles containing 25% phosphatidylserine (PS) and 4% PS was examined. The finding that  $K_d$  of LCh binding to vWf (3.8 nM) is 9.5 times higher than that of fVIII (0.4 nM), indicates that the heavy chain (HCh) is required for the maximal affinity of fVIII for vWf. In contrast, affinities of LCh for 25/75 PS/phosphatidylcholine (PC) monolayers and 4/76/20 PSPC-phosphatidylethanolamine (PE) vesicles are similar to that of fVIII, indicating that LCh is solely responsible for these interactions. It was also examined how removal of the acidic region affects the binding affinity of the remaining part of LCh for vWf and phospholipid. It was demonstrated that the loss of the LCh acidic region upon thrombin cleavage leads to an 11 and 160-fold increase in the dissociation rate constant ( $k_{off}$  value) and a 165 and 1500-fold increase in the  $K_d$  value of the binding of fVIII fragment A3–C1–C2 to vWf compared to that of LCh and fVIII, respectively. In contrast, the binding affinity of A3–C1–C2 for PS-containing membranes was 8–11-fold higher than that of LCh. Possible conformational change(s) in C2 domain upon removal of the acidic region were studied using anti-fVIII monoclonal antibody NMC-VIII/5 with an epitope within the C2 domain of LCh as a probe. The determined lower binding affinity of A3–C1–C2 for NMC-VIII/5 immobilized to a sensor chip than that of LCh, indicates that these conformational changes do occur. © 1999 Elsevier Science B.V. All rights reserved.

**Keywords:** Von Willebrand factor; Factor VIII; Membranes; Surface plasmon resonance detection; Detection, LC; Proteins; Phospholipids

### 1. Introduction

The plasma glycoprotein factor VIII (fVIII) functions as a cofactor for the factor X activation

\*Corresponding author. Tel.: +1-301-738-0750; fax: +1-301-738-0794.

complex (factor Xase) in the intrinsic pathway of blood coagulation [1]. Within the factor Xase complex, thrombin-activated factor VIII (fVIIIa) associated with membranes of activated platelets [2,3] or with synthetic phospholipid vesicles [4] binds to factor X [5] and to activated factor IX [4,6]. Activation of factor X by the fVIIIa/fIXa complex assembled on a phospholipid membrane is 100 000-fold more efficient than in the absence of phospholipid [7].

The fVIII protein consists of homologous A and C domains and a unique B domain which are arranged in the order A1–A2–B–A3–C1–C2 [8]. It is processed to a series of Me<sup>2+</sup> linked heterodimers produced by cleavage at the B–A3 junction [9], generating a light chain (LCh) consisting of the acidic region (AR) and A3, C1 and C2 domains and a heavy chain (HCh) which consists of the A1, A2, and B domains.

The site involved in the fVIII binding to synthetic phospholipid vesicles or platelets was localized within the C2 domain residues 2303–2332 [10]. The presence of at least 8% phosphatidylserine (PS) is required for the fVIII binding to synthetic PS phosphatidylcholine (PC) membranes [11]. Additional presence of phosphatidylethanolamine (PE) induces high affinity binding sites for fVIII on phospholipid membranes with physiologic (<8%) mole fractions of PS [12].

Maintenance of a normal fVIII level in the circulation is dependent on its complex formation with von Willebrand factor (vWf). When fVIII is bound to vWf, a stable association of its HCh and LCh is maintained [13], and fVIII is prevented from binding to phospholipid vesicles [14], platelets [15] or factor IXa, functions required for its procoagulant activity. In addition, vWf protects fVIII from activation by activated factor X [16] and from protein C catalyzed inactivation [14]. FVIII binds to vWf through LCh [17,18]. It was demonstrated that the C2 domain region 2303–2332, corresponding to the fVIII phospholipid binding site [10], is involved in fVIII interaction with both phospholipid and vWf. The importance of the LCh acidic region for the fVIII binding to vWf was suggested by the observations that several anti-acidic region monoclonal antibodies (mAbs) with epitopes within residues 1670–1689 [19,20] inhibit the fVIII binding to vWf, as does

complete deletion of the acidic region [21]. In addition, cleavage of LCh at Arg<sup>1689</sup> releases the acidic region residues 1649–1689 and leads to dissociation of fVIIIa from vWf [18,22,23].

Activation of fVIII by thrombin cleavage at Arg<sup>372</sup>, Arg<sup>740</sup> and Arg<sup>1689</sup> [24], results in at least a 100-fold increase of cofactor activity. The product, thrombin activated fVIII (fVIIIa), is a A1/A2/A3–C1–C2 heterotrimer [25] in which domains A1 and A3 retain the metal ion linkage and this stable dimer A1/A3–C1–C2 [26] is weakly associated with the A2 subunit mainly through electrostatic forces [25]. Spontaneous dissociation of the A2 subunit from the dimer results in non-proteolytic inactivation of fVIIIa.

The aim of the present study was to elucidate the roles of the acidic region and the C2 domain of LCh in binding to two major fVIII ligands, vWf and phospholipid. We developed surface plasmon resonance-based assays for detection of interaction between fVIII and its derivatives with vWf or PS-containing monolayers and intact synthetic vesicles. In these assays, LCh and its thrombin cleaved version A3–C1–C2 were used for quantitative measurements of their binding to vWf and to synthetic phospholipid surfaces in order to elucidate the role of the acidic region in both processes. The physiological relevance of the observations made using synthetic phospholipid membranes was validated by examination of the role of the acidic region of LCh in binding to activated platelets, which membranes serve as a surface for fVIII binding in vivo. The possibility that the conformational change(s) occur in the C2 domain upon removal of the acidic region of the LCh [27] was also examined using anti-C2 domain monoclonal antibody (mAb) as a probe.

## 2. Experimental

### 2.1. Monoclonal antibody

mAbs NMC-VIII/5 (epitope, C2 residues 2170–2327 [28]) and C4 (epitope, residues 1670–1784 [29]) were kindly provided by Drs. M. Shima (Nara Medical College, Japan) and Carol Fulcher (Scripps Clinic and Research Foundation, La Jolla, CA, USA), respectively. The anti-A2 mAb 8860 was

generously provided by Baxter/Hyland (Glendale, CA, USA). The preparation of IgG from mAbs NMC-VIII/5 and C4 was performed as described previously [28].

## 2.2. Protein purification

Plasma fVIII was purified from therapeutic concentrates of Method M (American Red Cross, Rockville, MD, USA) [30]. HCh and LCh were prepared as previously described [27]. Residual HCh was removed from the LCh preparation by its passage over a column with immobilized mAb 8860. A3–C1–C2 was prepared by cleavage of LCh with thrombin [31] and purification by ion exchange chromatography on a Resource S column (Pharmacia, Uppsala, Sweden) [32]. Traces of uncleaved LCh were removed by incubation for 18 h at 4°C in TBS, 5 mM CaCl<sub>2</sub>, 0.01% (v/v) Tween 20 with the anti-acidic region mAb C4 immobilized on CNBr-activated Sepharose 2B resin (Pharmacia) at 1.4 mg/ml. The final A3–C1–C2 preparation (3700 nM) contained <0.03 nM LCh, as measured by enzyme-linked immunosorbent assay described below. vWf was purified from cryoprecipitate (Cutter Biological, Berkeley, CA, USA) [33].

## 2.3. Enzyme-linked immunosorbent assay

Detection of residual uncleaved LCh in the A3–C1–C2 preparation was performed as follows. Immulon I plates (Dynatech Labs., Chantilly, VA, USA) were coated with 5 µg/ml mAb C4, blocked with 200 µl/well TBS, 2% bovine serum albumin (BSA), and LCh (0.025–1.25 nM) standards or A3–C1–C2 were added. All incubation steps were at 37°C for 1 h with shaking, and wells were washed three times with 200 µl TBS, 0.05% Tween 20 (Bio-Rad, Hercules, CA, USA). Bound LCh was detected with biotinylated mAb ESH8 followed by streptavidine-alkaline phosphatase. The color developed by alkaline-phosphatase cleavage of *p*-nitrophenyl phosphate was read at 410 nm in an MR5000 microtiter plate reader (Dynatech Labs.). Wells coated with mAb C4 and containing all components except LCh were used as negative controls. The average values of these controls were ≤10% of the maximal signal,

and they were subtracted from the values for all other samples.

## 2.4. Quantification of proteins

Concentrations of antibody and vWf were determined by the method of Bradford [34]. Concentrations of plasma-derived fVIII, LCh and HCh were determined by absorbance at 280 nm, using extinction coefficients of 1.2 [35], 1.34 [18] and 1.0 [18], respectively. The molar concentrations of fVIII, LCh and A3–C1–C2 were calculated using molecular masses of 300 kDa [8], 80 kDa [36] and 73 kDa [37], respectively. As the B domain is partially proteolyzed, the average molecular mass of 136 kDa for the HCh [36] was used.

## 2.5. Protein–protein binding using surface plasmon resonance

The kinetics of protein–protein interaction were determined by surface plasmon resonance using the IAsys instrument (Bisons, Cambridge, UK). vWf (50 µg/ml) or NMC-VIII/5 (50 µg/ml) in 10 mM sodium acetate, pH 5.0 or 4.5, respectively, were covalently coupled to the activated carboxymethyl-dextran (CMD) coated sensor cuvette (Bisons) via amino groups using succinimide ester chemistry [38]. Binding was measured in 200 µl TBS, pH 7.4, 5 mM CaCl<sub>2</sub>, 0.01% Tween 20 at 37°C for all ligands. Dissociation was initiated by substitution with the same buffer (200 µl) lacking ligand, which was changed with fresh buffer at a flow rate 10 µl/min. To regenerate the cuvette, complete dissociation of ligands bound to immobilized vWf was achieved by addition of 20 mM Tris, 0.35 M CaCl<sub>2</sub>, 0.6 M NaCl, 0.01% Tween 20, pH 7.2, for 2 min. Complexes of mAb NMC-VIII/5 with LCh or A3–C1–C2 were completely dissociated by addition of 0.1 M glycine, pH 3.0, for 3 min. Identical signals for reference binding of LCh to immobilized vWf or NMC-VIII/5 were obtained before and after a series of 25 regenerations.

## 2.6. Preparation of phospholipid vesicles

Phospholipids PS, PC and PE were purchased from Sigma (St. Louis, MO, USA), and biotin–LC–

dipalmitoyl PE (biotin–LC–DPPE) from Pierce (Rockford, IL, USA). Phospholipid vesicles with various PS, PC and/or PE content and vesicles containing biotin–LC–DPPE (0.5%) were prepared as described [39].

### 2.7. Protein–phospholipid binding measurements using surface plasmon resonance

The kinetics of protein–phospholipid interaction were determined by surface plasmon resonance using the Backer instrument (Backer, Uppsala, Sweden) or IAsys instrument (Bisons). Binding and subsequent dissociation was measured in HBS, pH 7.4, 5 mM CaCl<sub>2</sub> at 22°C for all ligands.

A supported PSPC or PC monolayer was formed on the surface of an HPA hydrophobic chip (Backer) by incubation of unilamellar PSPC (25/75) or 100% PC vesicles at 400 µg/ml in HBS for 20 min at 22°C, which produced a signal of 1100 RU. The phospholipid coated chip was blocked by 0.1 mg/ml BSA for 20 min. Binding of fVIII and its derivatives to a supported PSPC or PC monolayer was measured using the Backer instrument, where 1 ng of protein bound per mm<sup>2</sup> of the sensor chip produces a resonance signal of 1000 resonance units (RU). To regenerate the cuvette, complete dissociation of bound ligands was achieved by addition of 10 mM NaOH for 30 s.

Binding to intact vesicles was measured using the IAsys instrument, where 1 ng of protein bound per mm<sup>2</sup> of the sensor chip produces a signal of 600 RU. Biotin-coated cuvettes (Affinity Sensors, Cambridge, United Kingdom) were incubated with 20 µg/ml of streptavidin (Sigma) for 10 min, followed by the addition of biotinylated PSPCPE (4/76/20) or PCPE (80/20) vesicles at 200 µg/ml for 10 min. The resonance response due to binding of biotinylated phospholipid vesicles was 1000 Arc s. To regenerate the cuvette, complete dissociation of the biotin/streptavidin complex was achieved by addition of 5 M NaOH for 2 min.

### 2.8. Calculation of the kinetic parameters from surface plasmon resonance data

The values of the rate constants for the dissociation ( $k_{\text{off}}$ ) of fVIII and its derivatives from vWf or

monolayers and immobilized small vesicles were determined by fitting the dissociation kinetics data to the following equation describing a single phase dissociation process:

$$dR/dt = -k_{\text{off}}R \quad (1)$$

Where the surface plasmon resonance signal observed,  $R$ , is proportional to the formation of a complex between immobilized component and added ligand. It was shown [40] that

$$dR/dt = k_{\text{on}}CR_{\text{max}} - (k_{\text{on}}C + k_{\text{off}})R \quad (2)$$

where  $R_{\text{max}}$  is the maximal binding capacity of the immobilized ligand surface expressed in resonance units (RU) and  $C$  is the concentration of polypeptide in solution.

The  $k_{\text{on}}$  values were determined from individual association kinetics data using the integrated form of the rate Eq. (2):

$$R = \frac{Ck_{\text{on}}R_{\text{max}}[1 - e^{-(Ck_{\text{on}} + k_{\text{off}})t}]}{Ck_{\text{on}} + k_{\text{off}}} \quad (3)$$

The values of  $k_{\text{on}}$  and  $R_{\text{max}}$  were derived from nonlinear regression analysis by fitting  $R$  versus  $t$  to Eq. (3). The value of the  $k_{\text{off}}$  constant used in Eq. (3) was derived from the dissociation kinetics data fitted to Eq. (1). The values of equilibrium dissociation constants ( $K_d$ ) were calculated as  $k_{\text{off}}/k_{\text{on}}$ . All the fitting procedures were performed using Sigmaplot 1.02 (Jandel Scientific). All the values of the kinetic parameters are the mean ± standard deviation of the values derived from 3–4 independent kinetic measurements.

### 2.9. Determination of the binding affinity of fVIII, LCh and A3–C1–C2 for activated platelets

The binding affinities of fVIII or its fragments to activated platelets were determined by homologous or heterologous ligand displacement assays. <sup>125</sup>I-fVIII (0.25 nM) and increasing concentrations of unlabeled fVIII, LCh, A3–C1–C2 or HCh were incubated with activated platelets in Tyrode's solution at 22°C for 30 min. Aliquots (75 µl) from the samples were loaded onto 20% sucrose (350 µl) and centrifuged for 1 min at 10 000 g. Negative controls contained unactivated platelets and all the other

components. The negative control values ( $\leq 5\%$  of the maximal binding values) were subtracted from average values of triplicates of all other samples. For heterologous ligand displacement studies, the data were analyzed using model which assumes two distinct equilibria,  $R+L_1 \rightleftharpoons RL_1$  and  $R+L_2 \rightleftharpoons RL_2$ , where  $R$  is the concentration of fVIII binding sites on activated platelets,  $L_1$  is  $^{125}\text{I}$ -fVIII, and  $L_2$  is C2, LCh or A3–C1–C2. These equilibria are described by the equilibrium constants  $K_d$  and  $K_i$ , respectively. The data of homologous and heterologous displacements were fitted to a model assuming a single class of fVIII binding sites on activated platelets using the LIGAND program.

### 3. Results

#### 3.1. Use of surface plasmon resonance for elucidation of the LCh role in fVIII binding to vWf and phospholipid

To determine whether LCh is solely responsible for the high affinity fVIII interaction with vWf, kinetics of fVIII and LCh binding to and dissociation from vWf immobilized on a sensor cuvette using an IAsys instrument were compared. Representative curves in Fig. 1A show the resonance response reflecting the time course of fVIII or LCh association with immobilized vWf. Similar binding to a control

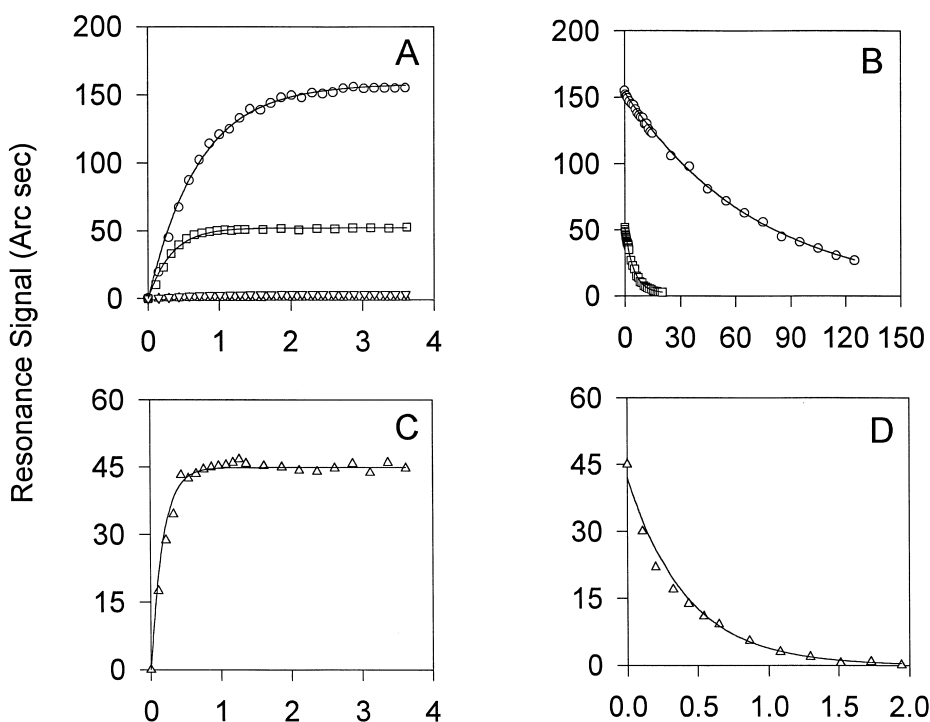


Fig. 1. Determination of the kinetic parameters of fVIII and LCh interaction with vWf using IAsys instrument. (A) Association of fVIII and LCh with vWf. vWf was immobilized to a sensor cuvette at  $5 \text{ ng/mm}^2$  of cuvette surface. The kinetics of  $50 \text{ nM}$  each fVIII ( $\circ$ ) and LCh ( $\square$ ) association with vWf was studied. The open symbols are data points selected from the sensograms. The solid lines show the best fit of the experimental association kinetic data to a model describing single phase association process (see Experimental section, Eq. (3)). Binding of  $50 \text{ nM}$  each fVIII ( $\nabla$ ) or LCh ( $\triangle$ ) to a control sensor (Fisons) cuvette without immobilized vWf was measured as above. (B) Dissociation kinetics of fVIII/vWf ( $\circ$ ) and LCh/vWf ( $\square$ ) complexes were recorded after replacement of the ligand solution with dissociation buffer, which was continuously changed with a fresh buffer at a flow rate  $10 \mu\text{l/min}$ . The solid lines show the best fit of the experimental data to Eq. (1), describing single phase dissociation to a baseline (see Experimental section). Association of  $400 \text{ nM}$  each A3–C1–C2 ( $\triangle$ ) with immobilized vWf (C) and dissociation of the corresponding complexes (D) was measured and fitted curves were obtained as above.

cuvette lacking vWf by maximal concentrations of fVIII or LCh gave resonance signals  $\leq 4\%$  of those in the presence of vWf (Fig. 1A) indicating the absence of nonspecific interactions with the cuvette.

The dissociation rate constants ( $k_{\text{off}}$ ) values were derived from the dissociation curves for fVIII and LCh (Fig. 1B) using Eq. (1) (Experimental section). The values of second order association rate constants ( $k_{\text{on}}$ ) were determined from the best fit of association kinetics data to the Eq. (3) describing single phase association (Experimental section).

The  $k_{\text{off}}$  for the fVIII/vWf complex ( $(2.3 \pm 0.6) \times 10^{-4} \text{ s}^{-1}$ ) was 14.8-fold lower than that for the LCh/vWf complex ( $(3.4 \pm 0.8) \cdot 10^{-3} \text{ s}^{-1}$ ), whereas the  $k_{\text{on}}$  values for these complexes were similar ( $(6.4 \pm 0.27) \cdot 10^5 \text{ M}^{-1} \text{ s}^{-1}$  and  $(9 \pm 0.5) \cdot 10^5 \text{ M}^{-1} \text{ s}^{-1}$ , respectively). The  $K_{\text{d}}$  for fVIII/vWf binding in the above experiments ( $0.4 \pm 0.095 \text{ nM}$ ) was similar to that of 0.2–0.46 nM determined in previous studies [15,20,41] and 9.5 fold higher than that of LCh ( $3.8 \pm 0.64 \text{ nM}$ ), suggesting that HCh is involved in fVIII/vWf binding. Since it was previously shown that HCh up to 2  $\mu\text{M}$  does not bind vWf [27], participation of HCh in fVIII binding to vWf is indirect.

To determine whether LCh is entirely responsible for the high affinity fVIII interaction with phospholipid membranes, we compared the binding affinities of LCh and fVIII for immobilized phospholipid monolayers or intact phospholipid vesicle. We initially determined parameters of LCh and fVIII binding to immobilized PSPC (25/75) monolayer, since synthetic membranes of this phospholipid composition were commonly used in previous fVIII binding studies [4,11,42,43]. It was previously shown that these monolayers represent a stable and structurally defined lipid environment resembling cell membranes [44]. The  $k_{\text{off}}$  values derived for fVIII and LCh from the dissociation curves shown in Fig. 2B were  $(1.44 \pm 0.05) \cdot 10^{-3} \text{ s}^{-1}$  and  $(1.65 \pm 0.03) \cdot 10^{-3} \text{ s}^{-1}$ , correspondingly. The  $k_{\text{on}}$  determined for fVIII and LCh from the representative association kinetic curves (Fig. 2A), were  $(6.3 \pm 0.6) \cdot 10^5 \text{ M}^{-1} \text{ s}^{-1}$  and  $(6.8 \pm 0.8) \cdot 10^5 \text{ M}^{-1} \text{ s}^{-1}$ , respectively. The respective  $K_{\text{d}}$  values for fVIII and LCh were  $2.2 \pm 0.21 \text{ nM}$  and  $2.3 \pm 0.26 \text{ nM}$ .

To elucidate if LCh is also entirely responsible for fVIII binding to *synthetic* membranes containing PS,

PC and PE at molar fractions similar to those in membranes of activated platelets [12], kinetic parameters for fVIII and LCh interaction with *synthetic* membranes containing 4% PS, 76% PC and 20% PE were compared. In this experiment small immobilized PSPCPE (4/76/20) vesicles were used. These vesicles were demonstrated to be a physiologically relevant model, since fVIII binding characteristics for such vesicles are comparable to those of platelet-derived microparticles [2]. Kinetics of fVIII and LCh association with and dissociation from immobilized small PSPCPE (4/76/20) vesicles (Fig. 2C and D, respectively) were optimally described by assuming one single class of binding sites on the vesicle for each ligand. The  $k_{\text{on}}$  values for fVIII [ $(2.3 \pm 0.26) \cdot 10^5 \text{ M}^{-1} \text{ s}^{-1}$ ] and LCh ( $(2.6 \pm 0.3) \cdot 10^5 \text{ M}^{-1} \text{ s}^{-1}$ ] derived from association curves (Fig. 2C) using Eq. (3), were 2.7 and 2.6 fold lower than the respective values for fVIII and LCh binding to a PSPC monolayer (Fig. 2A). In contrast, the  $k_{\text{off}}$  values for fVIII and LCh dissociation from PSPCPE vesicles [ $(1.7 \pm 0.2) \cdot 10^{-3} \text{ s}^{-1}$  and  $(1.8 \pm 0.04) \cdot 10^{-3} \text{ s}^{-1}$ , respectively] were similar to those determined above for their dissociation from PSPC (25/75) monolayers. Thus, a decrease in the membrane content of PS from 25% to 4% reduces only the rate of fVIII or LCh association with the membrane but does not affect the dissociation rates determined from Fig. 2B and D.

### 3.2. Effect of fluid-phase vWF and anti-C2 domain antibody on fVIII binding to vWf to phospholipid

It was previously demonstrated that anti-C2 domain antibody NMC-VIII/5 with an epitope within residues 2170–2327 inhibited both fVIII binding to phospholipid vesicles [45] and to vWf [28]. It was also shown previously, that fluid-phase vWf compete with immobilized phospholipids or vWf for fVIII binding [33]. To evaluate whether inhibition of the plasmon resonance-based fVIII/vWf and fVIII/phospholipid binding assays by fluid-phase antibodies and vWf can be used for determination of their concentrations, the effect of NMC-VIII/5 and vWf on fVIII binding to vWf and PSPCPE (4/76/20) was tested in the above assays. As seen from Fig. 3A and B, respectively, fluid-phase NMC-VIII/5 and vWf

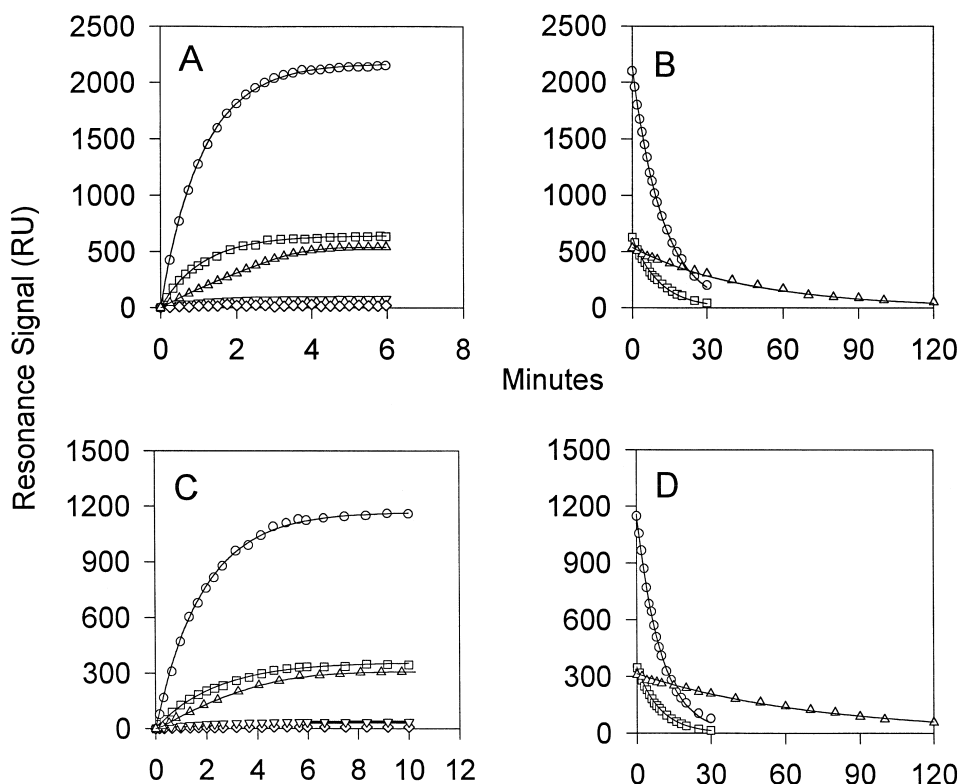


Fig. 2. Determination of the kinetic parameters of fVIII, LCh and A3–C1–C2 interaction with PSC (25/75) monolayers or PSCPCE (4/76/20) vesicles. (A) The kinetics of 24 nM fVIII ( $\circ$ ), LCh ( $\square$ ) or A3–C1–C2 ( $\triangle$ ) association with a PSC (25/75) monolayer prepared as described in the Experimental section was measured at the ligand 10  $\mu$ l flow rate using Biacore instrument. The open symbols are data points selected from the sensograms and the solid lines show the best fit of the experimental association kinetic data to a model describing a single phase association process (see Experimental section, Eq. (3)). In the control experiment, binding of 24 nM LCh ( $\diamond$ ) or A3–C1–C2 ( $\nabla$ ) to immobilized 100% PC (1000 RU/mm<sup>2</sup>) was measured as above. (B) The kinetics of fVIII ( $\circ$ ), LCh ( $\square$ ) or A3–C1–C2 ( $\triangle$ ) dissociation from the monolayers were recorded after replacement of the ligand solution with dissociation buffer, which was continuously changed at a flow rate of 10  $\mu$ l/min. The solid lines show the best fit of the experimental data to Eq. (1), describing single phase dissociation to a baseline (see Experimental section). (C) The kinetics of 24 nM of fVIII ( $\circ$ ), LCh ( $\square$ ) or A3–C1–C2 ( $\triangle$ ) association with PSCPCE (4/76/20) vesicles performed at a mixing speed of 40 rpm/min using IA sys instrument. The vesicles containing 0.5% biotin–LC–dipalmitoyl PE were immobilized as described in the Experimental section. In the control experiment, binding of 24 nM LCh ( $\diamond$ ) or A3–C1–C2 ( $\nabla$ ) to immobilized PCPE (80/20) vesicles was measured as above. (D) The kinetics of fVIII ( $\circ$ ), LCh ( $\square$ ) or A3–C1–C2 ( $\triangle$ ) dissociation from monolayers were recorded after replacement of the ligand solution by dissociation buffer using a mixing rate of 40 rpm/min.

inhibit fVIII binding to immobilized vWf or PSCPCE vesicles. The  $I_{50}$  concentrations were determined as described [46] by fitting inhibition data shown in Fig. 3 to the equation  $\%fVIII = 100 \times [1 - 1/(I + I_{50})]$ , where  $\%fVIII$  is the binding of fVIII in the presence of antibody or vWf expressed as a percentage of fVIII binding when no antibody or vWf was added. The respective  $I_{50}$  values for inhibition of fVIII binding to vWf and PSCPCE by NMC-VIII/5, derived from inhibition curves shown in Fig. 3A, were

$15.3 \pm 1.31$  and  $40.6 \pm 1.87$  nM. The  $I_{50}$  values for inhibition of fVIII binding to vWf and PSCPCE by vWf, derived from inhibition curves shown in Fig. 3B, were 15.3 and 29.6 nM, respectively. As follows from Fig. 3A and B, the 50% inhibition of fVIII binding to vWf and to immobilized vesicles by NMC-VIII/5 occurs at the antibody/fVIII molar ratios 0.55 and 0.6, which are similar to the respective values of 0.7 and 0.48 determined in the previous studies using enzyme-linked immuno-

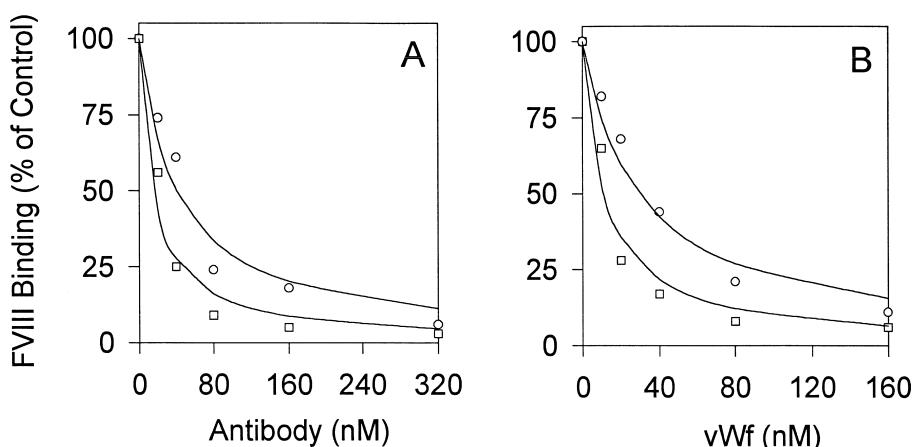


Fig. 3. Effect of mAb NMC-VIII/5 (A) and vWf (B) on the fVIII binding to immobilized vWf and PSCPE (4/76/20) vesicles. (A) Indicated concentrations of mAb NMC-VIII were preincubated with 50 nM fVIII (○) or 24 nM fVIII (□) for 15 min at 25°C, and the mixture (200 μl) was added to sensor chip with immobilized vWf (○) or PSCPE (4/76/20) vesicles (□) and equilibrium binding to immobilized vWf or PSCPE vesicles was measured as in Fig. 2A and C, correspondingly. The binding of fVIII in the presence of antibody is expressed as a percentage of fVIII binding when no antibody was added. (B) Indicated concentrations of vWf were preincubated with 50 nM fVIII (○) or 24 nM fVIII (□) for 15 min at 25°C, and the mixture was added to the sensor chip with immobilized vWf (○) or PSCPE (4/76/20) vesicles (□). FVIII binding in the presence of vWf was determined and expressed as in (A).

sorbent assay [47] or flow cytometry [45]. This suggests that fVIII binding to vWf and phospholipid in the developed surface plasmon resonance-based assays is specific and occurs with a stoichiometry similar to that observed in previously used fluid-phase fVIII binding assays [45,47].

### 3.3. Removal of the acidic region reduces the binding affinity of the remaining part of LCh for vWF but increases its affinity for phospholipid

Since LCh is responsible for fVIII binding to both vWf or phospholipid, surface plasmon resonance phenomenon was used to examine, whether the removal of the acidic region of LCh upon cleavage by thrombin at Arg<sup>1689</sup> affects the affinity of the remaining part of LCh (A3–C1–C2) for binding to PS-containing phospholipid membranes and to vWf. As seen from the kinetic curves (Fig. 1C), association of A3–C1–C2 with vWf approached equilibrium within 1.5 min. The  $k_{on}$  and  $k_{off}$  values for A3–C1–C2 derived from Fig. 1C and D, are  $(6.4 \pm 0.6) \cdot 10^4 M^{-1} s^{-1}$  and  $(4.0 \pm 0.7) \cdot 10^{-2} s^{-1}$ , respectively. The affinity of A3–C1–C2 interaction with vWf ( $K_d = 625 \pm 124$  nM) is 164-fold and 1560-fold lower than

that for LCh ( $K_d = 3.8 \pm 0.64$  nM) and fVIII ( $K_d = 0.4 \pm 0.095$  nM).

Since  $<0.003$  nM LCh was present in 400 nM A3–C1–C2 used in these experiments (see Experimental section), binding of 0.003 nM LCh to vWf was measured as a control, but none was observed during 2 min (data not shown). This indicates that A3–C1–C2 binding to vWf was not due to its contamination with residual acidic region in uncleaved LCh.

Kinetic curves for A3–C1–C2 interaction with PSC monolayers and PSCPE vesicles are shown in Fig. 2. The  $k_{off}$  values for A3–C1–C2 dissociation from PSC monolayer [ $(3.5 \pm 0.05) \cdot 10^{-4} s^{-1}$ ] or PSCPE vesicles [ $(2.3 \pm 0.09) \cdot 10^{-4} s^{-1}$ ] derived from the kinetic curves were 4.4 or 7.8 times lower than the respective values for the intact LCh. The  $k_{on}$  values for A3–C1–C2 association with the monolayer [ $(8.8 \pm 0.15) \cdot 10^5 M^{-1} s^{-1}$ ] or intact vesicles [ $(3.0 \pm 0.5) \cdot 10^5 M^{-1} s^{-1}$ ] determined from Figs. 2A and 3C, were similar to those for LCh [ $(6.8 \pm 0.8) \cdot 10^5$  and  $(2.6 \pm 0.3) \cdot 10^5 M^{-1} s^{-1}$ , correspondingly]. The  $K_d$  values for A3–C1–C2 binding to the monolayer or intact vesicles were 6–8 times lower than those for LCh.



### 3.4. The change in LCh binding affinity for vWF and phospholipid upon removal of the acidic region is related to conformational changes within the C2 domain

To test if the removal of the LCh acidic region leads to a conformational change(s) within the C2 domain, the affinities of LCh and A3–C1–C2 for immobilized anti-LCh mAb NMC-VIII/5 (epitope, within C2 domain residues 2170–2327) were compared. NMC-VIII/5 is known to inhibit fVIII binding to both vWf and phospholipid [28], which suggests that conformational change(s) in the C2 binding site for either ligand may be reflected by a change in the affinity for the antibody. The  $k_{on}$  and  $k_{off}$  values for LCh and A3–C1–C2 interaction with NMC-VIII/5 derived from the kinetic data shown in Fig. 4, were  $(1.03 \pm 0.12) \cdot 10^5 M^{-1} s^{-1}$  and  $(0.83 \pm 0.11) \cdot 10^5 M^{-1} s^{-1}$ , and  $(3.5 \pm 0.17) \cdot 10^{-5} s^{-1}$  and  $(4 \pm 0.3) \cdot 10^{-4} s^{-1}$ , respectively. The  $K_d$  value for LCh binding to NMC-VIII/5 ( $K_d = 0.34 \pm 0.045 nM$ ) is 14-fold lower than that for A3–C1–C2 ( $K_d = 4.8 \pm 0.73 nM$ ). The lower affinity of NMC-VIII/5 for A3–C1–C2 than that for LCh, suggests that the removal of the acidic region produces a conformational change(s) within the C2 domain. These changes are likely to affect the structure of vWf and phospholipid binding sites, since the epitope of

NMC-VIII/5 includes C2 domain amino-acid residues critical for fVIII binding to both ligands [28,47].

### 3.5. Determination of fVIII, LCh and A1–C1–C2 binding affinities for platelets in fluid phase

To examine if our observations made using synthetic phospholipid membranes are valid for membranes of platelets, we determined affinities of fVIII, LCh, and A3–C1–Ca–C2 for activated platelets using a heterologous displacement assay. In this assay, binding of  $^{125}I$ -labeled fVIII to activated platelets was competed by unlabeled fVIII and its fragments in the fluid phase (Fig. 5). The  $K_d$  value for fVIII binding to platelets ( $8.4 \pm 0.62 nM$ ) was calculated from the best fit of  $^{125}I$ -fVIII homologous displacement by unlabeled fVIII. Values of inhibition constants ( $K_i$ ) for LCh and A3–C1–C2 were calculated from heterologous displacement data using the LIGAND program and were  $7.7 \pm 1.2 nM$  and  $1.1 \pm 0.16 nM$ , respectively. Since the heterologous displacement experiments were performed at  $^{125}I$ -fVIII concentrations 30 times below  $K_d$  of fVIII binding to platelets, the  $K_i$  values determined for fVIII derivatives should be similar to  $K_d$  values for their direct binding to the activated platelets.

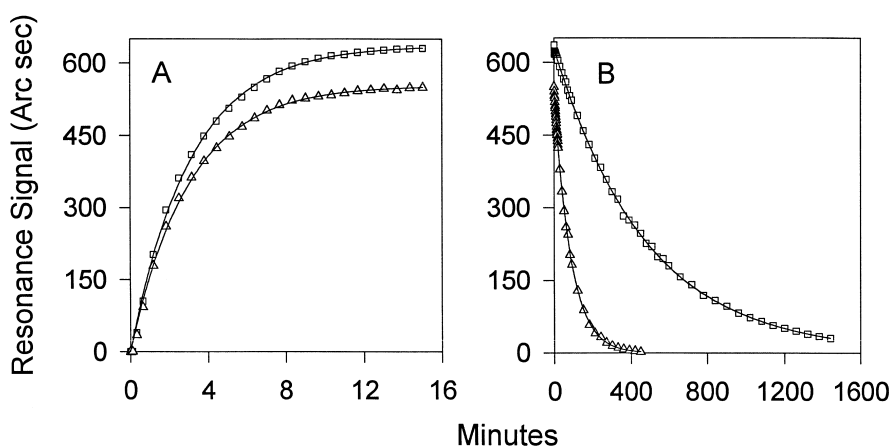


Fig. 4. The kinetics of binding of LCh, its derivatives and recombinant C2 domain to anti-C2 mAb NMC-VIII/5. Association of 40 nM each LCh ( $\square$ ) or A3–C1–C2 ( $\triangle$ ) with immobilized mAb NMC-VIII/5 ( $21 ng/mm^2$ ) (A) and dissociation of the corresponding complexes (B) was measured using IAsys instrument and fitted curves (solid lines) were obtained as in Fig. 1.

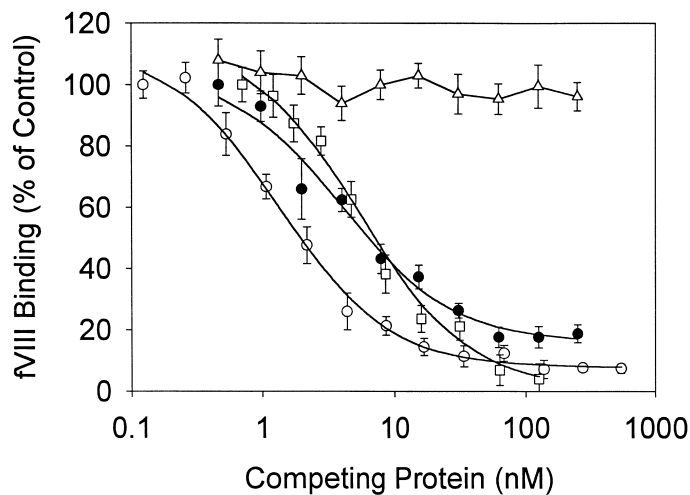


Fig. 5. Displacement of fVIII from platelets by its fragments.  $^{125}\text{I}$ -fVIII (0.25 nM) and activated platelets  $10^8/\text{ml}$  were incubated in the presence of varying concentrations of unlabeled fVIII ( $\square$ ), LCh ( $\circ$ ), A3-C1-C2 ( $\bullet$ ), or HCh ( $\triangle$ ), followed by the determination of  $^{125}\text{I}$ -fVIII binding (see Experimental section).  $^{125}\text{I}$ -fVIII binding to activated platelets in the presence of unlabeled competitor is expressed as the percentage of  $^{125}\text{I}$ -fVIII binding in the absence of competitor. Each point represents the mean value  $\pm$  S.D. of triplicates. The curves show a best fit of the data to a model describing heterologous ligand displacement for a single class of binding sites using the computer program LIGAND.

#### 4. Discussion

In the present study a surface plasmon resonance phenomenon was used to study interactions of a coagulation factor VIII (fVIII) with two physiologically important ligands, von Willebrand factor (vWf) and phospholipid. Two plasmon resonance based binding assays were developed for direct real-time kinetic measurements of the above interactions. Using these binding assays the role of the LCh in fVIII binding to vWf and to phospholipid was examined. As determined from the kinetic data shown in Fig. 1,  $K_d$  of LCh binding to vWf (3.8 nM) is 9.5 times higher than that of fVIII (0.4 nM), indicating that HCh is required for the maximal affinity of fVIII for vWf. A higher affinity of fVIII/vWf interaction than that of LCh/vWf is mainly due to a lower dissociation rate of the former complex. It is therefore possible that LCh has to be associated with HCh to acquire the optimal conformation for its binding to vWf. It was found, however, that the affinities of LCh for PSPC (25/75) monolayers and PSPCPE (4/76/20) vesicles, derived from the data in Fig. 2A–D are similar to that of fVIII, indicating that LCh is solely responsible for these interactions.

Using surface plasmon resonance, it was examined whether removal of the acidic region affects the affinity of the remaining part of LCh for binding to vWf and phospholipid. A high sensitivity of surface plasmon resonance and its capability to register fast dissociation kinetics shown in Fig. 1B, allowed us to determine a 1500-fold lower affinity of thrombin cleaved fVIII LCh (A3–C1–C2) than that of fVIII. From the data shown in Fig. 1, it was derived that the loss of the acidic region of LCh upon thrombin cleavage leads to a 11 and 160-fold increase in  $k_{\text{off}}$  and a 165 and 1500-fold increase in  $K_d$  of A3–C1–C2 binding to vWf compared to that of LCh and fVIII, respectively. This would predict that a similar reduction in fVIII affinity upon thrombin activation, allowing efficient fVIIIa binding to the phospholipid surface required for its maximal activity in the factor Xase enzyme complex. In contrast, from the kinetic data shown in Fig. 2 it was concluded, that removal of the acidic region leads to an 8–11-fold increase in the binding affinity of the remaining part (A3–C1–C2) for PS-containing synthetic membranes. The physiological relevance of this observation was supported by demonstration that the affinity of A3–C1–C2 for membranes of activated platelets is 8-fold

higher than that of the intact LCh. In addition, the binding affinities of fVIII, LCh and A3–C1–C2 for activated platelets ( $7.7 \pm 1.2$  nM,  $8.8 \pm 0.56$  nM and  $1.1 \pm 0.16$  nM, respectively) are similar to their affinities for synthetic PSPCPE (4/76/20) membranes ( $7.4 \pm 0.7$  nM,  $6.9 \pm 0.8$  nM and  $0.9 \pm 0.18$  nM, respectively). This further validates the use of synthetic phospholipid membranes as a physiologically relevant model of a phospholipid surface to the study kinetics of fVIII binding.

A high precision of plasmon resonance-based determinations allowed us to demonstrate that the acidic region of LCh may be required to maintain the conformation of the C2 binding site. This was done using mAb NMC-VIII/5, which prevents fVIII/vWf binding [28,47], as a probe to detect possible conformational changes in C2 upon removal of the acidic region. A considerably lower affinity of the thrombin cleaved LCh (A3–C1–C2) lacking the acidic region for binding to NMC-VIII/5 than that of LCh, determined from the kinetic data shown in Fig. 4, indicated that such changes occurs. It was hypothesized, therefore, that an increased affinity of A3–C1–C2 to phospholipid is related to conformational change(s) which occur within the C2 domain upon removal of the acidic region of the LCh [27].

The kinetic data shown in Fig. 2 could be interpreted assuming that the phospholipid binding site within C2 has two conformations: one which is capable of binding phospholipids with a lower affinity within fVIII and LCh and the other one with a higher affinity which exists in fVIIIa or in A3–C1–C2. It is not excluded, however, that the reduction of the overall negative charge of LCh upon removal of the acidic region may be partially responsible for the increased affinity of A3–C1–C2 for phospholipids as compared to LCh. Indeed, electrostatic forces are known to be involved in fVIII binding to PSPC vesicles [49], and removal of the acidic region 1649–1689 containing a high number of negatively charged residues would reduce the overall charge of LCh and the electrostatic repulsion between A3–C1–C2 and negatively charged PS. Since it is likely that the acidic region of LCh and the C2 domain are in close proximity [27,33], it would be expected that the removal of the LCh acidic region will increase the energy of C2 interaction with PS-containing synthetic membranes.

Since in the kinetic measurements performed in the present study, phospholipid monolayers or vesicles were immobilized to sensor chips, the kinetic parameters derived from these experiments may deviate from those determined in a fluid phase assay. The major source of such deviations could be a possible modification of a binding partner due to immobilization [50]. However, the  $K_d$  value of fVIII binding to vWf determined using plasmon resonance turned out to be similar to that previously determined in a fluid phase assay [15], indicating that vWf was not altered by immobilization.

The  $K_d$  value determined in this study for fVIII binding to immobilized PSPCPE (4/76/20) vesicles ( $7.4 \pm 0.7$  nM) is in good agreement with the  $K_d$  value determined in solution for fVIII binding to the vesicles of identical phospholipid composition (10.2 nM [12]). In addition, the association rate constant determined in the present study using plasmon resonance for fVIII binding to PSPC monolayer (25/75) ( $6.3 \times 10^5$  M<sup>-1</sup> s<sup>-1</sup>) was similar to the value of  $4.2 \times 10^5$  M<sup>-1</sup> s<sup>-1</sup> determined by Bardelle et al. [43] for fVIII association with small vesicles in fluid phase using a stopped-flow technique. The similarity of the parameters for fVIII/phospholipid binding previously determined by other methods and those determined in the present study using plasmon resonance indicate the validity of this technique for studying interactions of fVIII and its derivatives with phospholipids.

Thus, the monolayers formed on hydrophobic sensor chips or intact phospholipid vesicles immobilized to the sensor chips via biotinylated PE represent convenient and physiologically relevant models of phospholipid surfaces which can be used to study kinetics of interaction of fVIII or other coagulation proteins with phospholipids as well to model the assembly of the multi-protein complexes of the coagulation cascade on the phospholipid membranes. The examples of such complexes assembled on phospholipid membranes are the factor Xase complex consisting of factor VIIIa, factor IXa and factor X and the prothrombinase complex consisting of factor Va, factor Xa and prothrombin. The protein and protein phospholipid membrane interactions in these complexes are complicated. For instance, fVIIIa interacts with membrane-bound factor IXa with an affinity of 4 nM, and this affinity

increases by 10–15-fold [51] in the presence of factor X. The use of surface plasmon resonance for monitoring the assembly of multi-protein complexes on immobilized phospholipid surface, therefore, may allow to detect fine changes in membrane-binding or protein-binding affinity of any given protein constituting the above membrane-bound multi protein complexes upon addition of other components of the complex. There are several advantages of using plasmon-resonance technique for the above measurements, since neither phospholipid nor protein has to be labeled and immobilized synthetic phospholipid can be used repeatedly after regeneration. The reproducibility and accuracy can be assessed since the same phospholipid surface is used for multiple determinations. In addition, plasmon resonance can be used to detect the binding of any protein to phospholipid, whereas commonly used fluorescent measurements may not be possible if energy transfer is weak or does not occur. Furthermore, association and dissociation kinetic constants can be derived from plasmon resonance measurements allowing real-time detection of association and dissociation processes. These processes cannot be accurately measured by flow cytometry [47] or enzyme-linked immunosorbent assay [47].

The fVIII surface plasmon resonance-based binding assays may also be useful for analytical determinations, such as monitoring the fVIII concentration in the fractions obtained in a column chromatography. For this purpose, one will have to refer to a standard curve of equilibrium binding values obtained at varying concentrations of purified fVIII standard.

In addition, using the calibration curves shown in Fig. 3, it is possible to determine the vWf content in fVIII solution with known fVIII activity. In this determination, vWf-depleted fVIII preparation, which will have the clotting activity similar to that of sample of interest, will be used as a standard. The equilibrium binding of fVIII standard to vWf or phospholipid immobilized on the sensor chip will be measured as shown in Fig. 1A or Fig. 2A, C, and fVIII binding in the absence of vWf will be used as a control (100%). This will be followed by determination of the similar equilibrium binding of the fVIII sample containing the unknown concentration of vWf. The binding of the sample will be expressed as

a percentage of the control binding of the vWf-depleted standard, and the unknown vWf concentration will be determined using calibration curve similar to that shown in Fig. 3. This calibration curve will be prepared using vWf-depleted fVIII standard premixed with increasing concentrations of highly purified fVIII-depleted vWf.

## 5. Abbreviations

vWf,	von Willebrand factor
fVIII,	coagulation factor VIII
fVIIIa,	thrombin activated fVIII
LCh,	light chain of fVIII (fVIII residues 1649–2332)
HCh,	heavy chain of fVIII
A3–C1–C2,	thrombin cleaved LCh (fVIII residues 1690–2332)
AR,	the acidic region of the LCh (fVIII residues 1649–1689)
C2,	the C2 domain of the LCh, residues 2173–2332
mAb,	monoclonal antibody
PS,	phosphatidylserine
PE,	phosphatidylethanolamine
PC,	phosphatidylcholine
TBS,	Tris–buffered saline
HBS,	HEPES–buffered saline
HEPES,	4-(2-hydroxyethyl)-1-piperazineethanesulfonic acid
RU,	plasmon resonance units

## 6. United reference

[48]

## References

- [1] G. van Diejen, G. Tans, J. Rosing, H.C. Hemker, J. Biol. Chem. 256 (1981) 3433–3442.
- [2] G.E. Gilbert, P.J. Sims, T. Wiedmer, B. Furie, B.C. Furie, S.J. Shattil, J. Biol. Chem. 266 (1991) 17261–17268.
- [3] M.E. Nesheim, D.D. Pittman, J.H. Wang, D. Slonosky, A.R. Giles, R.J. Kaufman, J. Biol. Chem. 263 (1988) 16467–16470.

- [4] E.J. Duffy, E.T. Parder, V.P. Mutucumarana, A.E. Johnson, P. Lollar, *J. Biol. Chem.* 267 (1992) 17006–17011.
- [5] K. Lapan, P.J. Fay, *J. Biol. Chem.* 272 (1997) 2082–2088.
- [6] S.S. Ahmad, R. Rawala-Sheikh, P.N. Walsh, *J. Biol. Chem.* 264 (1989) 3244–3251.
- [7] G.E. Gilbert, A.A. Arena, *J. Biol. Chem.* 271 (1996) 11120–11125.
- [8] G.A. Vehar, B. Keyt, D. Eaton, H. Rodriguez, D.P. O'Brien, F. Rotblat, H. Oppermann, R. Keck, R.M. Lawn, D.J. Capon, *Nature* 312 (1984) 337–342.
- [9] P.J. Fay, M.T. Anderson, S.I. Chavin, V.J. Marder, *Biochim. Biophys. Acta* 871 (1986) 268–278.
- [10] M. Arai, D. Scandella, L.W. Hoyer, *J. Clin. Invest.* 83 (1989) 1978–1984.
- [11] G.E. Gilbert, D. Drinkwater, *Biochemistry* 32 (1993) 9577–9585.
- [12] G.E. Gilbert, A.A. Arena, *J. Biol. Chem.* 270 (1995) 18500–18505.
- [13] R.J. Wise, A.J. Dorner, M. Krane, D.D. Pittman, R.J. Kaufman, *J. Biol. Chem.* 266 (1991) 21948–21955.
- [14] P.J. Fay, J.V. Coumans, F.J. Walker, *J. Biol. Chem.* 266 (1991) 2172–2177.
- [15] M. Nesheim, D.D. Pittman, A.R. Giles, D.N. Fass, J.H. Wang, D. Slonosky, R.J. Kaufman, *J. Biol. Chem.* 266 (1991) 17815–17826.
- [16] S.J. Koppelman, J.A. Koedam, M. van Wijnen, D.M. Stern, P.P. Nawroth, J.J. Sixma, B.N. Bouma, *J. Lab. Clin. Med.* 123 (1994) 585–593.
- [17] R.J. Hamer, J.A. Koedam, N.H. Beeser-Visser, R.M. Bertina, J.A. van Mourik, J.J. Sixma, *Eur. J. Biochem.* 166 (1987) 37–43.
- [18] P. Lollar, D.C. Hill-Eubanks, C.G. Parker, *J. Biol. Chem.* 263 (1988) 10451–10455.
- [19] P.A. Foster, C.A. Fulcher, R.A. Houghten, T.S. Zimmerman, *Thromb. Haemostas.* 63 (1990) 403–406.
- [20] A. Leyte, M.P. Verbeet, T. Brodniewicz-Proba, J.A. van Mourik, K. Mertens, *Biochem. J.* 257 (1989) 679–683.
- [21] A. Leyte, H.B. van Schijndel, C. Niehrs, W.B. Huttner, M.P. Verbeet, K. Mertens, J.A. van Mourik, *J. Biol. Chem.* 266 (1991) 740–746.
- [22] S.S. Ahmad, R. Rawala-Sheikh, B. Ashby, P.N. Walsh, *J. Clin. Invest.* 84 (1989) 824–828.
- [23] D.C. Hill-Eubanks, C.G. Parker, P. Lollar, *Proc. Natl. Acad. Sci. USA* 86 (1989) 6508–6512.
- [24] D. Eaton, H. Rodriguez, G.A. Vehar, *Biochemistry* 25 (1986) 505–512.
- [25] P.J. Fay, P.J. Haidaris, T.M. Smudzin, *J. Biol. Chem.* 266 (1991) 8957–8962.
- [26] P. Lollar, C.G. Parker, *J. Biol. Chem.* 265 (1990) 1688–1692.
- [27] E.L. Saenko, D. Scandella, *J. Biol. Chem.* 272 (1997) 18007–18014.
- [28] M. Shima, D. Scandella, A. Yoshioka, H. Nakai, I. Tanaka, S. Kamisue, S. Terada, H. Fukui, *Thromb. Haemostas.* 69 (1993) 240–246.
- [29] P.A. Foster, C.A. Fulcher, R.A. Houghten, T.S. Zimmerman, *J. Biol. Chem.* 263 (1988) 5230–5234.
- [30] E.L. Saenko, M. Shima, G.E. Gilbert, D. Scandella, *J. Biol. Chem.* 271 (1996) 27424–27431.
- [31] L.M. Regan, P.J. Fay, *J. Biol. Chem.* 270 (1995) 8546–8552.
- [32] M. Nishino, J.P. Girma, C. Rothschild, E. Fressinaud, D. Meyer, *Blood* 74 (1989) 1591–1599.
- [33] E.L. Saenko, D. Scandella, *J. Biol. Chem.* 270 (1995) 13826–13833.
- [34] M.M. Bradford, *Anal. Biochem.* 72 (1976) 248–254.
- [35] P. Lollar, C.G. Parker, R.P. Tracy, *Blood* 71 (1988) 137–143.
- [36] P.J. Fay, *Arch. Biochem. Biophys.* 262 (1988) 525–531.
- [37] P.J. Fay, *Biochim. Biophys. Acta* 952 (1987) 181–190.
- [38] B. Johnsson, S. Lofas, G. Lindquist, *Anal. Biochem.* 198 (1991) 268–277.
- [39] Y. Barenholz, D. Gibbes, B.J. Litman, J. Goll, T.E. Thompson, F.D. Carlson, *Biochemistry* 16 (1977) 2806–2810.
- [40] D.J. O'Shannessy, M. Brigham-Burke, K.K. Sonenson, P. Hensley, I. Brooks, *Anal. Biochem.* 212 (1993) 457–468.
- [41] A.J. Vlot, S.J. Koppelman, J.C.M. Meijers, C. Damas, H.M. van den Berg, B.N. Bouma, J.J. Sixma, G.M. Willems, *Blood* 87 (1996) 1809–1816.
- [42] G.E. Gilbert, D. Drinkwater, S. Barter, S.B. Clouse, *J. Biol. Chem.* 267 (1992) 15861–15868.
- [43] C. Bardelle, B. Furie, B.C. Furie, G.E. Gilbert, *J. Biol. Chem.* 268 (1993) 8815–8824.
- [44] A.L. Plant, M. Brigham-Burke, E.C. Petrella, D.J. O'Shannessy, *Anal. Biochem.* 226 (1995) 342–348.
- [45] D. Scandella, G.E. Gilbert, M. Shima, C. Eagleson, M. Felch, R. Prescott, K.J. Rajalakshmi, E. Saenko, *Blood* 86 (1995) 1811–1819.
- [46] I.M. Lubin, J.F. Healey, R.T. Barrow, D. Scandella, P. Lollar, *J. Biol. Chem.* 272 (1997) 30191–30195.
- [47] E.L. Saenko, M. Shima, K.J. Rajalakshmi, D. Scandella, *J. Biol. Chem.* 269 (1994) 11601–11605.
- [48] D. Yeung, A. Gill, C.H. Maule, R.J. Davies, *Trends Anal. Chem.* 14 (1995) 49–56.
- [49] J.S. Atkins, P.R. Ganz, *Mol. Cell. Biochem.* 112 (1992) 61–71.
- [50] P.R. Edwards, A. Gill, V. Pollard-Knight, M. Hoare, P.E. Buckle, P.A. Lowe, R.J. Leatherbarrow, *Anal. Biochem.* 231 (1995) 210–217.
- [51] A. Mathur, D. Zhong, A.K. Sabharwal, K.J. Smith, S.P. Bajaj, *J. Biol. Chem.* 272 (1997) 23418–23426.